

Alteration of the magnetosphere of the Vela pulsar during a glitch

Jim Palfreyman^{1*}, John M. Dickey¹, Aidan Hotan², Simon Ellingsen¹ & Willem van Straten³

As pulsars lose energy, primarily in the form of magnetic dipole radiation, their rotation slows down accordingly. For some pulsars, this spin-down is interrupted by occasional abrupt spin-up events known as **glitches**¹. A glitch is hypothesized to be a catastrophic release of pinned vorticity² that provides an exchange of angular momentum between the superfluid outer core and the crust. This is manifested by a minute alteration in the rotation rate of the neutron star and its co-rotating magnetosphere, which is revealed by an abrupt change in the timing of observed radio pulses. Measurement of the flux density, polarization and single-pulse arrival times of the glitch with high time resolution may reveal the equation of state of the crustal superfluid, its drag-to-lift ratio and the parameters that describe its friction with the crust³. This has not hitherto been possible because glitch events happen unpredictably. Here we report single-pulse radio observations of a glitch in the Vela pulsar, which has a rotation frequency of 11.2 hertz. The glitch was detected on 2016 December 12 at 11:36 universal time, during continuous observations of the pulsar over a period of three years. We detected sudden changes in the pulse shape coincident with the glitch event: one pulse was unusually broad, the next pulse was missing (a ‘null’) and the following two pulses had unexpectedly low linear polarization. This sequence was followed by a 2.6-second interval during which pulses arrived later than usual, indicating that the glitch affects the magnetosphere.

In 2013 we began a three-year observing programme of the Vela pulsar with the aim of recording each single pulse during its next glitch (see Methods). On 2016 December 12 at 11:36 universal time (UT), a glitch of magnitude $\Delta\nu/\nu = 1.431 \times 10^{-6}$ (where $\nu = 11.2$ Hz is the rotation rate) was observed at both the 26-m telescope installed at Mount Pleasant, Tasmania, and the 30-m telescope at Ceduna, South Australia. Extended Data Table 1 shows the arrival times at the Solar System barycentre, as recorded by the two telescopes.

Figure 1 shows a plot of the arrival time residuals of single pulses recorded at Mount Pleasant over a time range of 72 min centred on the glitch. The residuals are the difference between the experimental data and the timing-model results for ν and $\dot{\nu}$, calculated using 36 min of single-pulse data obtained before the glitch.

The inset of Fig. 1 shows a magnification of the plot around the time of the glitch, t_g (vertical red line; see Methods). Near this time, three very-low-probability events occurred: (1) a ‘null’, which followed an unusually broad pulse, (2) a brief increase in the mean of the timing residuals, implying either a decrease in ν or, more probably, a change in the magnetosphere that affected timings, and (3) a reduction in the variance of the timing residuals.

Figure 2 shows 11 consecutive pulses including the ‘null’ that occurred at pulse number 77 (in the recorded file). Although pulses 72–75 look typical, pulse 76 looks different: the flux is spread smoothly over about 10 ms, the entire width of the integrated pulse profile of the Vela pulsar. We have not seen a similarly broad pulse shape in the more than 100,000 pulses that we have examined.

The pulse following this broad pulse is the ‘null’ pulse, and pulses 78 and 79 show minimal linear polarization, as demonstrated by the

absence of a position angle swing (right column of Fig. 2). Then, typical pulse shapes are again observed from pulse 80 onwards. Analysis of data collected on other days shows that on average, the single-pulse flux density is below the detection threshold of the 26-m telescope once every 77,700 pulses.

Although some pulsars show frequent null pulses, Vela does not^{4,5}, and general pulsar observations indicate that nulls are not expected to occur in young pulsars such as Vela⁶. We cannot determine whether pulse 77 in Fig. 2 is a true null, with zero flux emitted, a very faint pulse

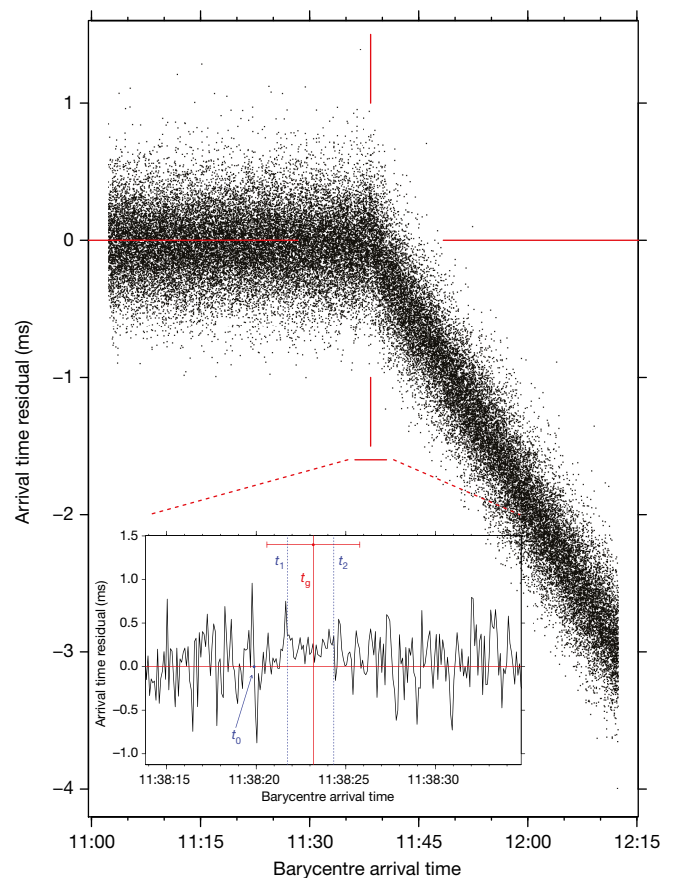


Fig. 1 | Timing residuals of single pulses near the time of the glitch.

The horizontal axis shows the arrival time at the Solar System barycentre on modified Julian day 57,734, and the vertical axis shows the residual of the arrival time, obtained from the pre-glitch model. The vertical red line marks the fitted time of the glitch (t_g). The inset shows a magnification of the plot. 3.3 s before t_g , a ‘null’ occurred (t_0), followed by an unusual change in the timing residuals, with late mean arrival times and reduced variances. Because the ‘null’ cannot be timed, it has been placed on the 0.0 ms line. The horizontal error bar represents the 1σ uncertainty in the fitting of t_g .

¹University of Tasmania, Sandy Bay, Tasmania, Australia. ²CSIRO Astronomy and Space Science, Kensington, Western Australia, Australia. ³Auckland University of Technology, Auckland, New Zealand. *e-mail: jim77742@gmail.com

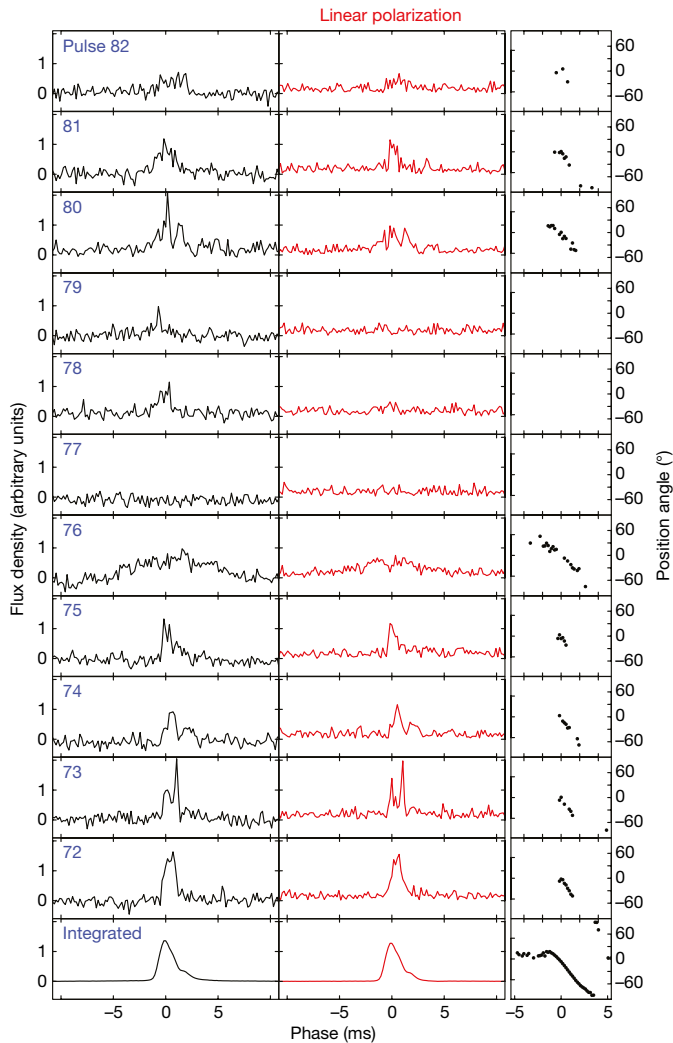


Fig. 2 | A contiguous sequence of single pulses surrounding the ‘null’. Each row corresponds to a single pulse, with time increasing from bottom to top and the pulse number (in the recorded file) indicated in blue. The ‘null’ is pulse 77. For reference, the bottom row shows the integrated pulse profile. The left panels show the total flux density in arbitrary units, the middle panels show linear polarization and the right panels show the position angle of the linear polarization. Circular polarization was negligible and is not shown. The slight offset in the linear polarization is due to off-pulse noise. Only about a fifth of the pulse period is shown. The position angle is not plotted for pulses 78 and 79 because no linear polarization was detected immediately after the ‘null’.

that is below the detection threshold of the 26-m telescope, or even a pulse with more severe broadening than pulse 76. However, such a pulse is a rare event. The ‘null’ pulse appears at time t_0 , only 3.3 s (37 pulsar rotations) before the best estimate of t_g , which has a 1σ uncertainty of 2.5 s. The probability of a null appearing anywhere in the 37 rotations before the glitch is $P = 4.8 \times 10^{-4}$.

Soon after the ‘null’, at $t_1 = t_0 + 1.8$ s (20 pulsar rotations), a substantial change occurred in both the mean and the variance of the timing residuals, which lasted for 2.6 s (29 pulsar rotations), until time t_2 . We searched two other full days of data (more than about 1.4×10^6 pulses) for a sequence of pulses of similar length and with a greater change in the mean, combined with a smaller change in variance than that observed here. None was found. Figure 3 shows a scatter plot of the mean and standard deviation (σ) of single pulses over the 36-min period before t_g , as shown in the left half of Fig. 1. This extraordinary offset in the mean arrival times of the sequence of pulses and the low corresponding variance suggest that the pulsar emission mechanism was affected by the glitch process during this interval.

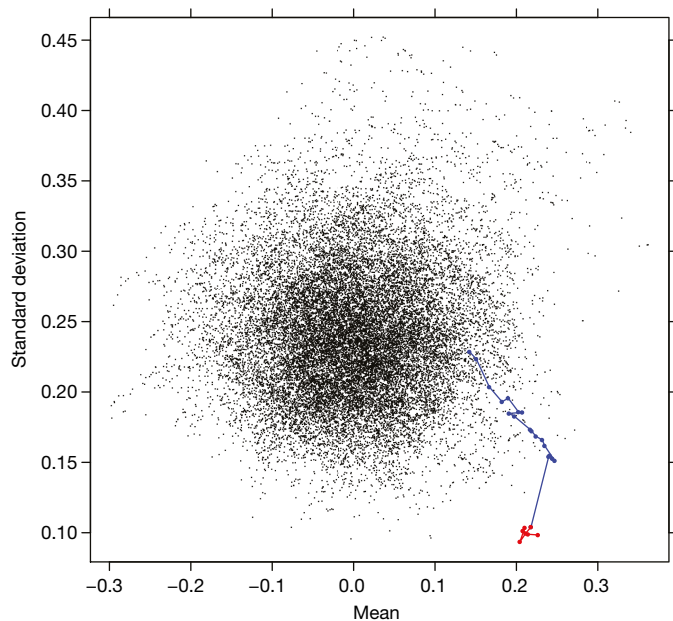


Fig. 3 | Scatter plot of the mean and standard deviation of single-pulse timing residuals. Data are shown for the 36 min leading up to the glitch (left half of Fig. 1), calculated using a sliding window of 21 data points. The blue dots correspond to the period t_0 – t_1 and the red outliers to t_1 – t_2 . The connecting lines show how the sequence progresses. The units are milliseconds.

Figure 4a shows a 260-s view of the timing residuals, with the ‘null’ at t_0 marked, Fig. 4b provides the cumulative sum of the timing residuals, and Fig. 4c shows the cumulative sum after glitch modelling has been applied to the 72 min of data. The cumulative sums highlight overall changes that are not apparent in the residual plot. The sequence of pulses showing increased mean and reduced variance commences at t_1 and finishes at t_2 . Label t_3 marks what appears to be a permanent speed-up in rotation after the glitch process has been completed.

We note that t_g can be fitted to a precision of only 2.5 s, but the ‘null’ pulse provides a fiducial time t_0 with a precision of the pulsar rotation rate, 89 ms. The timing of the spin-down, from t_1 to t_2 , is based on the sustained change in the mean and variance shown in the inset of Fig. 1. Extended Data Table 2 shows the arrival times of these events at the Solar System barycentre.

The 2.6 s from t_1 to t_2 could be associated with the unpinning process of superfluid vortices, and the associated changes in angular momentum, which are presumed to be the cause of pulsar glitches. An alternative explanation is changes in the magnetosphere triggered by the glitch. These changes could be caused by the unpinning of the vortices affecting the magnetic flux tubes in the core.

The 4.4-s interval (49 pulsar rotations) between t_0 and t_2 may indicate the rise time (τ_r) of the glitch, that is, the time required to transfer angular momentum from the superfluid-permeated inner crust to the outer crust. The rise time of the glitch has implications for the equation of state. Sourie et al.³ compare the predictions of two equations of state, the density-dependent hadronic (DDH) model and DDH δ , which takes into account a scalar isovector interaction channel. For a pulsar mass of $1.3 M_\odot$ – $1.6 M_\odot$, where M_\odot is the mass of the Sun, the DDH model predicts a glitch rise time of 4–5.5 s and DDH δ predicts 2.5–3.5 s. If τ_r is indeed 4.4 s, then DDH might be the preferred equation-of-state model.

The 43.8-s interval (490 pulsar rotations) between t_2 and t_3 may correspond to the time after the glitch when the crust and interior are synchronized, before their rotation rates become decoupled.

Sedrakian & Cordes⁷ present a model in which the crustal magnetic field provides a potential barrier against the superconducting proton vortices in the core, which in turn act as a barrier to the superfluid vortices that are trying to migrate outwards. On the basis of this model,

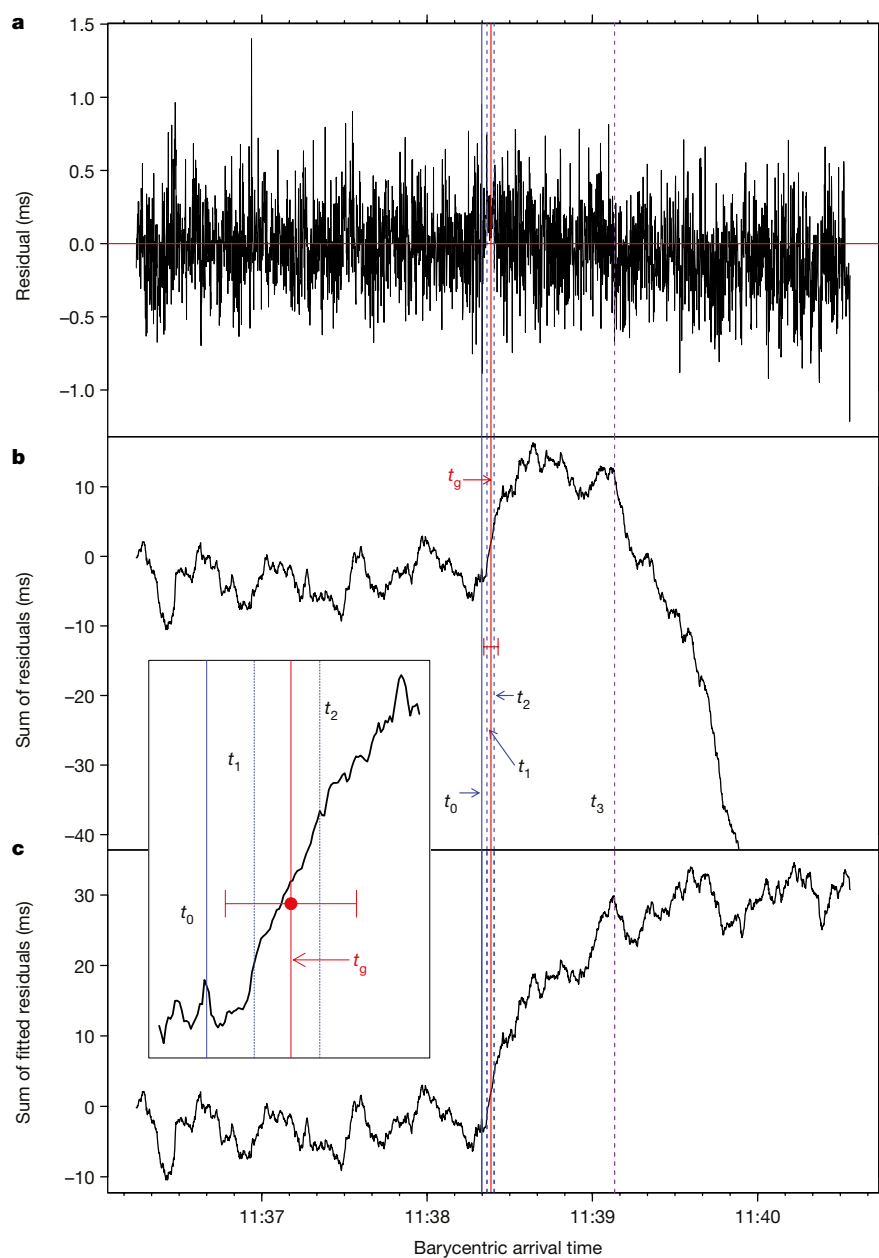


Fig. 4 | Timing residuals and their cumulative sum around the time of the glitch. Residuals are shown for the 260 s around the time of the glitch t_g (solid red line). **a**, Timing residuals (in milliseconds) similar to those of Fig. 1, with no glitch modelling applied. **b**, Cumulative sum of the timing residuals of **a**. **c**, Cumulative sum of timing residuals, after glitch modelling has been applied. The events observed at times t_0 – t_3 (see text) are highlighted. Inset, magnified view of **b** showing t_0 , t_1 , t_g and t_2 . The horizontal error bar represents the 1σ uncertainty in the fitting of t_g .

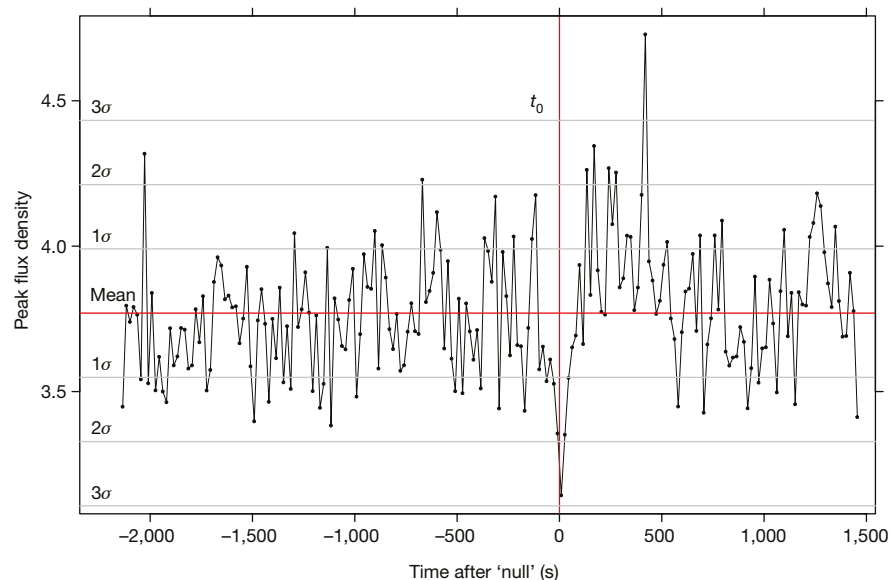


Fig. 5 | Peak flux density around the time of the 'null'. The flux density is shown in arbitrary units and the 'null' occurs at t_0 (vertical red line). Data have been binned into 200-pulse (about 18 s) bins. The horizontal lines indicate 1σ spacings.

they predict that a glitch would affect the geometry of the pulsar's magnetic field. This may be what we have observed in the 'null' pulse (pulse 77), the strange shape of pulse 76, and the loss of linear polarization in pulses 78 and 79.

We also observed a 3σ dip in the peak flux density for about 2 min on either side of t_0 (see Fig. 5). Vela is known⁸ to emit bright pulses that arrive between 1 ms and 1.5 ms before the main pulse. This 3σ dip, combined with the reduced variance of the timing residuals, suggests that fewer bright pulses were emitted from the magnetosphere in this interval. The disruption of the magnetosphere could have caused the normal coherent emission process to break down sufficiently to stop the emission of bright pulses from the precursor region, where they are usually seen. Changes in the particle bunching in the magnetosphere could affect coherence, the radio flux density, the beaming direction or the emission height.

Future observations of single pulses associated with glitches in Vela may provide confirmation that glitches consistently cause null pulses or peculiar-shaped pulses. Observations with larger telescopes (or telescope arrays) may probe this behaviour more deeply by determining whether the 'null' is genuine, which will help us to resolve some of the outstanding issues with regard to the internal mechanics and equations of state of neutron stars.

Online content

Any Methods, including any statements of data availability and Nature Research reporting summaries, along with any additional references and Source Data files, are available in the online version of the paper at <https://doi.org/10.1038/s41586-018-0001-x>.

Received: 12 July 2017; Accepted: 24 January 2018;

Published online 11 April 2018.

1. Rees, M. J. & Trimble, V. L. Physical sciences: planet, pulsar, "glitch" and wisp. *Nature* **229**, 395–396 (1971).
2. Anderson, P. W. & Itoh, N. Pulsar glitches and restlessness as a hard superfluidity phenomenon. *Nature* **256**, 25–27 (1975).

3. Sourie, A., Chamel, N., Novak, J. & Oertel, M. Global numerical simulations of the rise of vortex-mediated pulsar glitches in full general relativity. *Mon. Not. R. Astron. Soc.* **464**, 4641–4657 (2017).
4. Biggs, J. D. An analysis of radio pulsar nulling statistics. *Astrophys. J.* **394**, 574–580 (1992).
5. Johnston, S., van Straten, W., Kramer, M. & Bailes, M. High time resolution observations of the Vela pulsar. *Astrophys. J.* **549**, L101–L104 (2001).
6. Rankin, J. M. Toward an empirical theory of pulsar emission. III - mode changing, drifting subpulses, and pulse nulling. *Astrophys. J.* **301**, 901–922 (1986).
7. Sedrakian, A. & Cordes, J. M. Vortex-interface interactions and generation of glitches in pulsars. *Mon. Not. R. Astron. Soc.* **307**, 365–375 (1999).
8. Krishnamohan, S. & Downs, G. S. Intensity dependence of the pulse profile and polarization of the Vela pulsar. *Astrophys. J.* **265**, 372–388 (1983).

Acknowledgements We thank the staff at the School of Physical Sciences of the University of Tasmania who assisted in the observing programme. J.P. especially thanks B. Reid, E. Baynes and B. Bedson for on-site support at the 26-m and 30-m radio telescopes. J.P. also thanks N. Bochenek and W. Kean Tai for assisting in the searches of previous 'nulls'. We acknowledge the Australian Government Research Training Program Scholarship, which helped fund this research, and the Tasmanian Partnership for Advanced Computing (TPAC) at the University of Tasmania, which is funded by the Australian Government through its NCRIS and RDSI programmes, for use of the 2.3-PB storage facility.

Reviewer information *Nature* thanks J. Cordes and the other anonymous reviewer(s) for their contribution to the peer review of this work.

Author contributions J.P. conducted all the observations, led the analysis and the writing of the manuscript and produced all the plots. J.M.D. provided input on the manuscript and analysis. W.v.S. conducted the polarization calibration and assisted with the manuscript and analysis. S.E. and A.H. assisted with the manuscript and analysis.

Competing interests The authors declare no competing interests.

Additional information

Extended data is available for this paper at <https://doi.org/10.1038/s41586-018-0001-x>.

Reprints and permissions information is available at <http://www.nature.com/reprints>.

Correspondence and requests for materials should be addressed to J.P.

Publisher's note: Springer Nature remains neutral with regard to jurisdictional claims in published maps and institutional affiliations.

METHODS

Using the Mount Pleasant 26-m radio telescope, which is located near Hobart, Tasmania, we observed Vela when it was above the lower elevation limit, 4.3° , obtaining data for about 19 h each day. We also observed Vela with our 30-m telescope in Ceduna, South Australia. Both telescopes operated at a centre frequency of 1,376 MHz and a bandwidth of 64 MHz. Although the Ceduna dish is larger than that of the Mount Pleasant 26-m telescope, its receiver is much less sensitive because it is not cooled to cryogenic temperatures. Both telescopes have dual linearly polarized receivers.

We recorded about 14,000 h of baseband voltage data from Mount Pleasant in both polarizations at a rate of 128×10^6 samples per second. Data from the Ceduna telescope were recorded in a buffer and discarded until the glitch occurred.

The baseband data files from both observatories were coherently de-dispersed, detected and integrated into single pulses using DSPSR⁹. In the time domain, each rotation of the pulsar was divided into 8,192 phase intervals (giving a resolution of 10.9 μ s) and in the frequency domain, the 64-MHz band was divided into 16 sub-bands. PSRCHIVE¹⁰ was used for analysis, and polarization calibration was performed by using Vela as a polarized reference source, but using 128 frequency sub-bands and 1,024 phase intervals¹¹.

The glitch epoch (t_g) was calculated using the TEMPO2 software^{12,13} and a two-stage iterative process. First, we adjusted t_g to minimize the phase ($\Delta\phi$). We modelled for changes in ν and $\dot{\nu}$ and set the long-term glitch decay parameters¹⁴ to $\Delta\nu_d = 1.29 \times 10^{-7}$ and $\tau_d = 0.96$. Then, we used an iterative process and stopped when $\Delta\phi < 10^{-7}$ ($\Delta\phi = 6.98 \times 10^{-8} \approx 6$ ms).

After this approximation, we adjusted t_g manually to minimize the root-mean-square residuals in the arrival time (data minus model). Then, we adjusted ν to minimize the root-mean-square residuals, and then $\dot{\nu}$. This was repeated several times, until convergence was achieved. In each step of this process, the plot of the root-mean-square residuals was a parabola smooth enough to validate our best-fit determination.

The $\Delta\nu/\nu$ and $\Delta\dot{\nu}/\dot{\nu}$ values for the Mount Pleasant observations shown in Extended Data Table 1 were obtained using four days of data, whereas the fitting of the glitch epoch was based on 72 min of data. The corresponding results for Ceduna were based on 15 h of data, but with only about 1 h of pre-glitch timings available; thus, $\Delta\nu/\nu$ was not well constrained and $\Delta\dot{\nu}/\dot{\nu}$ could not be determined.

Data availability. Source Data files containing the data shown in the figures are available in the online version of the paper. The raw data were generated at the Mount Pleasant and Ceduna radio observatories, which are operated by the University of Tasmania, and are available from the corresponding author upon reasonable request.

Code availability. The software DSPSR, TEMPO2 and PSRCHIVE are available at <http://dpspr.sourceforge.net/>, <http://www.atnf.csiro.au/research/pulsar/tempo2/> and <http://psrchive.sourceforge.net/>, respectively.

- van Straten, W. & Bailes, M. DSPSR: digital signal processing software for pulsar astronomy. *Publ. Astron. Soc. Aust.* **28**, 1–14 (2011).
- Hotan, A. W., van Straten, W. & Manchester, R. N. PSRCHIVE and PSRFITS: an open approach to radio pulsar data storage and analysis. *Publ. Astron. Soc. Aust.* **21**, 302–309 (2004).
- van Straten, W. High-fidelity radio astronomical polarimetry using a millisecond pulsar as a polarized reference source. *Astrophys. J. Suppl. Ser.* **204**, 13 (2013).
- Hobbs, G. B., Edwards, R. T. & Manchester, R. N. TEMPO2, a new pulsar-timing package–I. An overview. *Mon. Not. R. Astron. Soc.* **369**, 655–672 (2006).
- Edwards, R. T., Hobbs, G. B. & Manchester, R. N. TEMPO2, a new pulsar timing package–II. The timing model and precision estimates. *Mon. Not. R. Astron. Soc.* **372**, 1549–1574 (2006).
- Sarkissian, J. M., Reynolds, J. E., Hobbs, G. & Harvey-Smith, L. One year of monitoring the Vela pulsar using a phased array feed. *Publ. Astron. Soc. Aust.* **34**, e027 (2017).

Extended Data Table 1 | Arrival times of the 2016 glitch of the Vela pulsar

| Location | MJD | Time (UTC) | $\frac{\Delta\nu}{\nu}$ | $\frac{\Delta\dot{\nu}}{\dot{\nu}}$ |
|--------------------|--------------------------|-------------|----------------------------|-------------------------------------|
| Mount Pleasant | 57734.484991 | 11:38:23.2 | 1431.24×10^{-9} | 9.2×10^{-3} |
| <i>uncertainty</i> | $\pm 2.9 \times 10^{-5}$ | ± 2.5 s | $\pm 0.069 \times 10^{-9}$ | $\pm 0.83 \times 10^{-3}$ |
| Ceduna | 57734.484973 | 11:38:21.7 | 1433.5×10^{-9} | N/A |
| <i>uncertainty</i> | $\pm 3.2 \times 10^{-5}$ | ± 2.8 s | N/A | N/A |

Arrival times at the Solar System barycentre were estimated on the basis of data recorded at each observatory. The last two columns list the relative change in rotation frequency and the relative change in the first derivative of the rotation frequency. Uncertainties are 1σ . MJD, modified Julian date; UTC, coordinated universal time.

Extended Data Table 2 | Arrival times of key events at the Solar System barycentre

| | Event | MJD | Time | Δt (s) | Rotations |
|-------|------------------|---------------|------------|----------------|-----------|
| t_0 | null pulse | 57734.4849521 | 11:38:19.9 | 1.8 | 20 |
| t_1 | spin-down starts | 57734.4849738 | 11:38:21.7 | 1.5 | 17 |
| t_g | glitch fit | 57734.4849906 | 11:38:23.2 | 1.1 | 12 |
| t_2 | spin-down ends | 57734.4850038 | 11:38:24.3 | 43.8 | 490 |
| t_3 | spin-up starts | 57734.48551 | 11:39:08.1 | | |

The times t_g and t_0 - t_3 are listed, as shown in Fig. 4. The last two columns list the time difference (Δt) and number of pulsar rotations between events. MJD, modified Julian date.